A New Method to Identify Nearby, Young, Low-mass Stars

David R. Rodriguez[1], M. S. Bessell[2], B. Zuckerman[1], Joel H. Kastner[3]

ABSTRACT

We describe a new method to identify young, late-type stars within ∼150 pc of the Earth that employs visual or near-infrared data and the GALEX GR4/5 database. For spectral types later than K5, we demonstrate that the ratio of GALEX near-ultraviolet (NUV) to visual and near-IR emission is larger for stars with ages between 10 and 100 Myr than for older, main sequence stars. A search in regions of the sky encompassing the TW Hya and Scorpius-Centaurus Associations has returned 54 high-quality candidates for followup. Spectroscopic observations of 24 of these M1–M5 objects reveal Li 6708Å absorption in at least 17 systems. Because GALEX surveys have covered a significant fraction of the sky, this methodology should prove valuable for future young star studies.

Subject headings: open clusters and associations: individual(Lower Centaurus–Crux, Upper Centaurus–Lupus, TW Hydrae) — stars: evolution — stars: pre-main sequence — ultraviolet: stars

1. Introduction

The last two decades have seen the discovery of a number of moving groups and associations near the Earth containing young stars with ages in the range ∼10 to 100 Myr (for reviews see Zuckerman & Song 2004 and Torres et al. 2008). By studying stars in these moving groups we can observe the evolution of stellar properties as a function of age. Identifying additional members, particularly fainter, low-mass stars, is key to understanding the processes involved in the earliest stages of stellar, substellar, and massive planet evolution.

[1]Dept. of Physics & Astronomy, University of California, Los Angeles 90095, USA (drodrigu@astro.ucla.edu)

[2]The Australian National University, Cotter Road, Weston Creek ACT 2611, Australia

[3]Center for Imaging Science, Rochester Institute of Technology, 54 Lomb Memorial Drive, Rochester NY 14623

Low-mass stars with ages ranging from 10–100 Myr are luminous sources of X-rays with respect to their bolometric luminosities (Kastner et al. 1997; Zuckerman & Song 2004; Preibisch & Feigelson 2005; Torres et al. 2006, and references therein). Several successful searches for nearby young stars exploited their characteristically large X-ray activities to identify promising candidates (Kastner et al. 1997; Song et al. 2003; Torres et al. 2006). In addition to X-ray activity, however, young low mass stars also exhibit larger chromospheric activity than their older counterparts (as measured by the R'_{HK} index; see Mamajek & Hillenbrand 2008 and references therein). Higher chromospheric activity is correlated with increased ultraviolet emission in stars (Walkowicz & Hawley 2009). Hence, when compared to the older population of low mass stars, young stars will stand out as being UV-bright (for example, see Figure 3 in Guinan & Engle 2009).

The Galaxy Evolution Explorer satellite (GALEX, Martin et al. 2005) has performed a number of large area surveys in the far-ultraviolet (FUV, 1344–1786Å) and near-ultraviolet (NUV, 1771–2831Å). The All-sky Imaging Survey (AIS), in particular, has covered ∼3/4 of the sky, and hence represents an excellent tool to identify UV-bright sources. However, in order not to damage its detectors, GALEX generally does not point within 10 degrees of the galactic plane. Even with this limitation, GALEX has already explored the regions covered by many nearby, young stellar associations (Zuckerman & Song 2004; Torres et al. 2008).

A previous study performed in the Taurus and Upper Scorpius regions used GALEX to identify candidate young stars (Findeisen & Hillenbrand 2010). However, these regions are populated by stars with ages ≤5 Myr. We have successfully applied a similar strategy (described in § 2) to search for nearby stars with ages 10–100 Myr and with spectral types later than K5 using archival data available in the GALEX GR4/5 data release.

2. Method

The search strategy we have employed consists of identifying UV-excess, late-type objects using NUV-Optical/NIR colors. With available proper motion data from the literature, we perform a UVW space velocity analysis and the best candidate objects are selected for spectroscopic followup. We describe our method in detail in Sections 2.1–2.3.

2.1. GALEX (UV-based) Identification of Candidate Nearby, Young Stars

To examine whether 10 to 100 Myr old stars stand out in the ultraviolet, we compare the absolute NUV magnitudes for stars in Torres et al. (2008), which lists members of many

of the young, nearby stellar associations, with the "Catalogue of Nearby Stars, 3rd Edition" by Gliese & Jahreiß (1991); most the latter are considerably older than a few 100 Myr. In particular, we used the catalog provided in Stauffer et al. (2010), which lists accurate coordinates for most of the stars in Gliese & Jahreiß (1991). To identify UV sources we make use of CasJobs[1], an interface to query the GALEX database. The results are displayed in Figures 1 and 2. It is clear from these figures that young stars stand out from the older population. In particular, stars with V–K$\gtrsim$3.5 ($\sim$M0) and ages as old as 70 Myr (the AB Dor group in Torres et al. 2008) are brighter in NUV than the older Gliese stars; the only exceptions are flare stars (from Gershberg et al. 1999 or SIMBAD) and some multiple systems (from Dommanget & Nys 2002 and Pourbaix et al. 2004). GALEX has a PSF FWHM of 5″ and, hence, cannot resolve binary systems with much smaller separations. Additionally, in some close binary systems (such as RS CVn-type systems) the component stars can interact with one another and may produce additional UV emission. The only exception to this trend of brighter NUV magnitudes for young stars is BD +01 2447, classified by Torres et al. (2008; see also references within) as an AB Dor member, with V–K$\sim$4.3, which we discuss later in § 3.4. Fig. 2, which displays NUV–V colors for these stars, also shows how young stars stand out. Reddening towards these objects can significantly affect the shorter wavelengths. Findeisen & Hillenbrand (2010) apply a reddening curve in which $A_{NUV}/A_V = 2.63$; however, using the reddening curve of Cardelli et al. (1989) and $R_V = 3.1$, we obtain $A_{NUV}/A_V = 2.96$. While most Gliese stars are within 25 pc, most of the young stars are more distant. Regardless of the exact value for A_{NUV}/A_V, extinction towards the younger, more distant objects will generally be higher than for the nearby Gliese stars. Thus the effect of extinction will be to bring the locus of the young star populations in Figs. 1 and 2 closer to the Gliese old star locus. That is, the intrinsic separation in absolute NUV magnitude and in NUV–V between young and old stars is, if anything, somewhat greater on average than indicated in Figs. 1 and 2.

Young, early-M stars in these associations (with ages 10–30 Myr) tend to have absolute NUV magnitudes between 15–16 (see Fig. 1). The 3-σ sensitivity for the GALEX AIS survey is 22.0 magnitudes for each 100-second exposure, which means that these young stars could be detected at the 3-σ level out to at least 160 pc. Findeisen & Hillenbrand (2010) estimate that GALEX can detect unextincted photospheres of K5 stars out to 140 pc with 300-second exposures, implying absolute NUV magnitudes of about 17. Mid-K stars with ages of 70 Myr, however, have absolute NUV magnitudes generally brighter than 15, suggesting that even at 70 Myr, these stars will be about 2 magnitudes brighter than their older counterparts (as illustrated in Fig. 1 at V–K$\sim$3). As previously mentioned, extinction towards these

[1]http://mastweb.stsci.edu/gcasjobs/

objects will cause them to have redder NUV–V colors— similar to that of older field stars. Extinction of (at least) $A_V \sim 0.7$ magnitudes would be required for 70 Myr-old mid-K stars to have NUV magnitudes comparable to equally distant, but older, mid-K stars.

To see if these 10–100 Myr-old systems also stand out as UV-bright in GALEX-2MASS colors, and to carry out a pilot study for the feasibility of a large scale program, we examine a region of sky encompassing the TW Hya Association (TWA). After defining a suitable search region (see Table 1), we select all objects detected in NUV (our initial search of the TW Hya Association also required detection in FUV). These sources are then cross-matched with the 2MASS Point Source Catalog (Cutri et al. 2003) with a matching radius of $2''$, somewhat larger than the GALEX pointing uncertainty ($\sim 1''$, Morrissey et al. 2007). This allows us to produce color-color plots like the one in Figure 3. In these plots, galaxies tend to lie in a well defined region of space (between about 0.5<J–K<2 and 2<NUV–J<7) while stars follow a diagonal line from J–K$\sim$0 and NUV–J$\sim$2 to J–K$\sim$1 and NUV–J$\sim$13. The black symbols in Figure 3 are the TWA stars from Torres et al. (2008), all of which lie below the stellar sequence; TW Hya is the object with NUV–J$\sim$6. The stellar locus is well defined by an average of the relations in Findeisen & Hillenbrand (2010; see their Equation 2) and we have plotted this as a solid line in Figure 4. Also shown are the 10–100 Myr old stars, which can again be distinguished from older field stars in that they lie below the stellar sequence (i.e., they have UV excesses). The thick solid line represents the best linear fit to the locus of young stars, and illustrates the difference between the young and old stellar populations, particularly for the lower mass stars (J–K $\geq$ 0.7). While the separation is not as pronounced as in the NUV–V plots, clearly these diagrams should enable one to select candidate young, low-mass stars using only GALEX and 2MASS colors.

In Figures 3 and 4, the young stars of the TWA all lie below the stellar sequence. However, there is some scatter, and not every object with UV excess will be a young star. For example, flare stars are known contaminants in young star X-ray searches, and the same is true for our UV-selection methods (see also Figs. 1 and 2). We select objects with UV excesses similar to those of the known young stars (defined algebraically by NUV–J $\leq$ 10.20(J–K) + 2.2) and J–K between 0.7 and 1, as most M-type stars have J–K colors of about 0.8. Our selection criteria is illustrated in Figure 5 along with our candidate objects (see § 3) and fits to the old and young stellar locus as described above (see also Fig 4).

2.2. Proper Motions and UVW Space Velocities

To distinguish between candidate young stars and other UV excess sources, we make use of proper motion information available in the literature. In particular, we use the USNO-B1

(Monet et al. 2003), UCAC3 (Zacharias et al. 2010), and PPMX (Röser et al. 2008) proper motion catalogs, which can be accessed from the TOPCAT[2] Virtual Observatory tool. In some cases we also check the PPMXL catalog (Roeser et al. 2010). Our UV excess sources are matched against all three catalogs, compared with proper motions of members in the association of interest, and then merged while removing duplicate entries. In cases where one catalog has a proper motion that is discrepant from the others, we favor the proper motions listed in UCAC3 and PPMX.

We next estimate galactic space velocities (UVW) for candidate stars. This step requires estimates for distances and radial velocities. In order to obtain photometric distances, we estimate spectral types using available broadband photometry (for example, data from DENIS (DENIS Consortium 2005) or the proper motion catalogs listed above). From the spectral type we estimate photometric distances using empirical and theoretical isochrones for young stars of ages 10 and 100 Myr (Song et al. 2003; Zuckerman & Song 2004, and references therein). Because nearly all candidates lack radial velocities, we use these distance estimates (along with the positions and proper motions) to estimate Galactic UVW with respect to the Sun for a range of velocities extending from −80 to 80 km/s. Zuckerman & Song (2004) define a "good UVW box" that contains nearly all young stars. If any object has UVW within this box, that is, UVW within 0 to −15, −10 to −34, and +3 to −20 km s^{-1}, they are flagged for followup. In this case U is defined as positive towards the Galactic center.

Follow up for all candidates so identified involves first checking against known association members. In the TWA, for example, nearly all known members are recovered via the above methodology, including some that are not included in Torres et al. (2008) but are present in older compilations, such as those in Zuckerman & Song (2004). The candidates are searched in SIMBAD as well, though most have no SIMBAD entry and only limited information in VizieR.

2.3. Lithium Line Spectroscopy

Candidates considered for spectroscopic followup are those with a broad range of radial velocities that would give UVW velocities consistent with nearby, young star status and photometric distances consistent with other members in the association of interest. The presence and strength of Li 6708Å absorption in the spectrum can indicate whether or not the object is young (see Figure 3 in Zuckerman & Song 2004, and the associated discussion in § 5.1 of the same paper). A high-resolution spectrum can also be used to determine the

[2]Available at http://www.starlink.ac.uk/topcat/

radial velocity of the candidate object, which can then be used to better constrain its UVW velocities.

Although the presence of Li for stars of the spectral types of interest (K5 and later) is a strong indication of youth, lithium burning is very sensitive to stellar mass (and thus spectral type). For example, β Pic Moving Group stars ($\sim$12 Myr) of spectral types M3–4 show very little Li in their spectra (Song et al. 2002; Zuckerman & Song 2004; Yee & Jensen 2010). Hence, a non-detection of lithium absorption does not immediately imply the system is old, particularly for later M spectral types. As demonstrated by Yee & Jensen (2010), lithium depletion models tend to predict much weaker Li absorption at any given age. Using such models would yield far greater ages for $\sim$12 Myr M3.5–M5 stars. Because many of our candidates fall in this range, a non-detection would imply a system is older than about 10 Myr, but does not provide an upper limit to this age. Such a system could, however, still be a member of a young association. In such cases, membership could be confirmed via accurate distance, proper motion, and radial velocity measurements.

3. Application: Identification of Nearby Young Stars in and near the TW Hya Association

3.1. NUV/NIR-based Candidate Identification

We have used the method described in Section 2 to perform a search for young stars in the TW Hya Association (TWA, $\sim$8 Myr, 40–60 pc; Zuckerman & Song 2004; Torres et al. 2008, and references therein) and the Scorpius–Centaurus region (Preibisch & Mamajek 2008). The Sco–Cen region is divided into a number of associations: Upper Scorpius (US, $\sim$5–6 Myr old), Upper Centaurus-Lupus (UCL, $\sim$14–15 Myr), and Lower Centaurus-Crux (LCC, $\sim$11–12 Myr), which are located about 120–140 pc distant (Preibisch & Mamajek 2008)[3]. In order to limit our searches to a manageable number of objects (the GALEX catalog CasJobs search interface has built-in memory limits), we divided the Sco–Cen search into a set of 4 RA/Dec centroids, each with a given radius (see Table 1 and Fig. 6). There is some overlap between these regions, so the resulting lists of objects (after cross-correlating with 2MASS) were merged and duplicate entries were removed. Candidate objects were selected via the technique described in Sections 2.1 and 2.2.

We identified $\sim$150 promising candidates through this methodology. In order to select

[3]Based on Li abundances in late-type members of LCC and UCL, Song, Bessel, & Zuckerman (unpublished) suggest these regions are only $\sim$10 Myr old.

the best objects to observe, we selected only those with a broad range of possible radial velocities that would give UVW consistent with those of young stars, and those with distances comparable to that of the TWA or Sco–Cen regions. After these cuts we had selected 10 TWA candidates and 44 Sco–Cen candidates. These 54 candidates are listed in Table 2, with spectral types estimated from photometric colors. These candidate objects are also displayed in Figure 5 along with known TWA members for comparison. Note, however, that the LCC and TWA are very close in the sky and have similar ages, so accurate distances are needed to determine in which association these targets belong. The TWA and Sco–Cen search fields are displayed in Figure 6, with candidate objects shown as open circles and those for which we obtained spectra (Table 3) shown as filled circles.

3.2. Spectroscopic Followup

To check for signatures of youth, such as the presence of lithium absorption at 6708Å, we obtained R=3000 spectra of the 24 stars listed in Table 3 with the Wide Field Spectrograph (WiFeS) at the Siding Springs Observatory's 2.3-m telescope during 2010 March and 2010 May. We also acquired R=7000 spectra for five of our objects in 2010 August. Four of these targets were selected in our TWA search and 20 in our Sco–Cen searches, though a few Sco–Cen candidates overlap with the TWA search region (see Fig 6). WiFeS (Dopita et al. 2007) is a double–beam, image–slicing integral field spectrograph, and provides a 25×38 arcsec field with $0.5''$ pixels. A variety of gratings can be used to provide R=3000 and R=7000 spectra over optical wavelengths. We used the B_{3000} and R_{3000} gratings to cover the wavelength range from 3200Å to 9800Å. The spectra for the region covering Hα and Li 6708Å are displayed in Figures 7 and 8. We have measured equivalent widths of Hα, He I, and Li I for these objects (when detected) and summarize these values in Table 3. Spectral types listed in Table 3 are estimated using the TiO5 index as described in Reid et al. (1995), with an estimated precision of ± 0.5 in subclass.

3.3. Results and Discussion

Of the 24 targets listed in Table 3, 17 display evidence of Li absorption at 6708Å. The remaining 7 have no Li or an unidentified weak/moderate feature is present at a slightly bluer wavelength (offset by 2–3Å). Those objects with the weak feature near Li were re-observed with R=7000 (see below). Note, however, that all systems with no evidence of Li in their spectra have spectral types M3.5–M4.5. As previously mentioned, stars of these spectral types will burn lithium in as little as $\sim$10 Myr such that a lack of lithium does not

immediately imply the system is old. Of those that do display some lithium absorption, 6 are M1–M3, with the remaining being later than M3.5. Those later than M3.5 must be at most ∼10 Myr old in order to show such strong lithium absorption. The earlier M-types will burn their lithium somewhat more slowly, so these systems may be of age ∼10 Myr.

X-ray detection has been one way young stars have been identified (for example, Kastner et al. 1997; Song et al. 2003; Torres et al. 2006). Only 5 of our 24 spectroscopic targets (and only 14 among the 54 candidates) have ROSAT All-Sky Survey (RASS) X-ray detections within 1′ of the target's 2MASS coordinates in either the Bright or Faint source catalogs. The lack of X-ray detection in RASS suggest these objects, if they are young, are producing too little X-ray emission to be readily detected at these distances. Table 2 lists L_X/L_{bol} for all candidates, including upper limits for RASS non-detections (assuming a RASS flux limit of 2×10^{-13} ergs cm^{-2} s^{-1}; Schmitt et al. 1995). All RASS-detected candidates have log $L_X/L_{bol} \sim -3$, which is typical of nearby M-stars (see Fig. 5 in Riaz et al. 2006).

Hα equivalent widths (EW) is one way that T Tauri stars are identified and classified. For these spectral types, values for Hα EW ≥10–20Å are typically observed in classical T Tauri stars (White & Basri 2003). Of the stars observed spectroscopically, 9 show Hα EW larger than 10Å, with a 10th system having an Hα EW consistent with 10Å. In addition to Hα, we also measure He I EW at 5876Å and 6678Å in those systems with clear He I emission. The 8 systems with measured He I also have strong Hα. Of these, 3 have no lithium absorption detected, but have spectral types M3.5–M4. The detected He I and lack of Li may suggest these systems are young, but somewhat older than ∼10 Myr. We comment on several noteworthy targets below for which we acquired R=7000 spectra.

2M1125–44: This is an M4 star detected in our TWA search, with a photometric distance of 75 pc if 10 Myr-old. The R=3000 spectrum suggested a dip near 6708Å, but a higher resolution spectrum revealed no detectable Li, though He I emission lines at 5876 and 6678Å are detected. The radial velocity for this system (19.5 ± 2 km s^{-1}; S. Murphy, private comm.), combined with the 10 Myr-old photometric distance estimate, provide UVW that are consistent with those of young stars. At a distance of 75 pc, the Galactic UVW are -4 ± 5, -23 ± 3, -4 ± 5 km s^{-1}. The lack of Li, however, implies that the star is older than ∼10 Myr, but even at ∼30 Myr (implying a closer distance of about 50 pc) the UVW are still consistent with those of a young star (-1 ± 4, -22 ± 2, -1 ± 4 km s^{-1}). This star has been detected in X-rays by the ROSAT All Sky Survey and has log $L_X/L_{bol} \sim -2.33$. Hence, this candidate is possibly a young star based on dynamics and X-ray emission, though is not likely to be a member of the ∼8 Myr TWA. The UVW is marginally consistent with that of TWA (−11, −18, −5 km s^{-1}; Zuckerman & Song 2004) and the Sco-Cen region (UCL: −6.8, −19.3, −5.7, LCC: −8.2, −18.6, −6.4, with dispersions of 3–7 km s^{-1}; Sartori et al. 2003).

A parallax measurement will be key in determining the age of this object and membership in any nearby association.

2M1226–33: This is an M5 star detected in our TWA search with a photometric distance of 65 pc if 10 Myr-old. This system has very strong Hα and He lines. The Hα has equivalent width of 64 ± 4Å and the 5876Å and 6678Å He I lines have EWs ∼6Å and ∼1Å, respectively. Strong lithium absorption is also observed (410 mÅ). The presence of such strong lines suggests the system may be a classical T Tauri star (White & Basri 2003). We obtained an additional spectrum for this star using R=7000. The equivalent widths differ somewhat from the R=3000 spectrum and are listed as an additional row in Table 3. White & Basri (2003) find that Hα full widths at 10% higher than 270 km s^{-1} are found among classical T Tauri stars. With the higher resolution spectrum, we measured a full width at the 10% level for Hα of 300 km s^{-1}, suggesting this object could be a nearby classical T Tauri system. Comparison with Figure 3 in Natta et al. (2004) suggests an accretion rate of $\sim 10^{-10}$ $M_\odot$ yr^{-1}. With the higher resolution spectrum, we were also able to determine a radial velocity of 14.8 ± 3 km s^{-1}. We calculate UVW of -8 ± 3, -24 ± 4, -1 ± 3 km s^{-1}. The UVW is marginally consistent with that of TWA and Sco-Cen. There is no RASS detection for this object implying $\log L_X/L_{bol} < -3.10$; the field has not been observed with Chandra or XMM.

2M1450–34, 2M1508–34, & 2M1524–29: The R=3000 spectra for these three stars had an absorption feature near lithium, but offset by 2–3Å from the expected 6708Å. A higher resolution spectrum reveals no clear signature of lithium, though a blended ∼100 mÅ feature is seen in 2M1524–29 at a wavelength of 6707.1Å (see Figure 8). 2M1450–34's R=3000 spectrum shows possible He I emission at 6678Å, but this is not seen in the R=7000 spectrum (the R=7000 spectrum does not cover the region where He I 5876Å can be seen in emission). The radial velocities measured from the R=7000 spectrum are 7.3, 4.9, and 6.0 km s^{-1}, (all with uncertainties of ±3 km s^{-1}) for 2M1450–34, 2M1508–34, and 2M1524–29, respectively. With 10 Myr photometric distance estimates, the UVW for 2M1450–34 are: -5 ± 3, -29 ± 6, -6 ± 3 km s^{-1}; for 2M1508–34: -7 ± 3, -29 ± 6, -5 ± 3 km s^{-1}; and for 2M1524–29: -1 ± 3, -23 ± 5, -3 ± 3 km s^{-1}. Both 2M1450–34 and 2M1508–34 have UVW that appear to be marginally consistent with those of TWA and Sco-Cen. None of these objects have detections in RASS (note that all three stars have photometric distances larger than 100 pc, see Table 2), nor have they been observed by Chandra or XMM.

3.4. Two Stars with Unusual NUV–J Color

While carrying out the search described in Sections 3.1–3.3, we found two systems in Torres et al. (2008) with particularly unusual NUV–V and NUV–J colors (Figs. 2 and 4):

BD +01 2447: This M2 star is listed in Torres et al. (2008) as an AB Dor Association member (age 70 Myr). BD +01 2447, also known as HIP 51317, is 7 pc away, with an upper limit of 60 mÅ for Li EW (Zickgraf et al. 2005). For an M2 star, however, lithium may be depleted within ∼12 Myr (see Fig. 3 in Zuckerman & Song 2004). The kinematics of the system are consistent with membership in the AB Dor Association and X-ray emission has been detected (log $f_X/f_V \sim -3.53$; Zickgraf et al. 2005). This object has a 2MASS K magnitude of 5.311, which (at 7 pc) corresponds to M_K of 6.1. The models of Baraffe et al. (1998) predict an M2 star would reach such an M_K in about 80–100 Myr. These results are consistent with this being a nearby AB Dor member. However, in Figures 1, 2, and 4, this system is located in the region of color-color (and color-magnitude) space more common for older systems. It is noteworthy that, of all of the ≤70 Myr stars in Torres et al. (2008) detected by GALEX, BD +01 2447 is the only star (excepting TW Hya, see below) that lies significantly outside the locus of young stars. BD +01 2447 also displays slow rotation ($v \sin i < 3$ km s^{-1}), which is more commonly seen in older systems (T. Forveille 2010, private communication). A closer examination of BD +01 2447 is warranted so as to understand its weak NUV emission.

TW Hya: This star, namesake of the TW Hya Association, stands out in all our NUV figures due to its substantial NUV excess. In particular, it has NUV–J∼6, while the rest of the TWA stars have NUV–J∼9–11. If the UV excesses displayed by the TWA stars can be ascribed to chromospheric activity due to their youth, an additional emission source is required to explain why TW Hya is ∼3 magnitudes brighter in NUV than the rest of the TWA. Of the young stars plotted on our figures, TW Hya is the only known classical T Tauri star. The most likely explanation for the increased UV emission is ongoing accretion onto the star, as suggested by its optical and X-ray emission properties ($\sim 10^{-8}\ M_\odot\ yr^{-1}$, Kastner et al. 2002). Additionally, the orientation of the system is such that we are seeing its accretion unobscured (the disk is near face-on, Krist et al. 2000). Our unobscured view of the accretion onto this star is therefore the likely explanation for its high UV flux. This suggests that, barring intervening absorbing material, actively accreting stars such as TW Hya will readily stand out in GALEX-Optical/NIR colors.

4. Conclusions

We have demonstrated a new technique based on GALEX and 2MASS colors that can readily identify young, low-mass stars near the Earth. Findeisen & Hillenbrand (2010) similarly demonstrated that such a UV/near-IR search strategy is feasible for stars younger than ∼5 Myr, but essentially no such stars are known to exist within ∼100 pc of Earth. The present study demonstrates that GALEX NUV fluxes may be used in conjunction with either optical or near-IR fluxes to identify nearby stars with ages in the range 10–100 Myr and spectral types K5 or later. With additional information, namely space velocities, we have formulated an efficient method to identify candidate members of nearby stellar associations.

We have performed a search in the TWA and Sco–Cen region and recovered 54 high-quality candidates. Of these, we observed 24 spectroscopically and detected lithium absorption, an indicator of youth, in at least 17 M1–M5 systems. Those with no lithium absorption have spectral types M3.5–M4.5, a range where lithium is believed to be depleted within ∼10 Myr (Song et al. 2002; Zuckerman & Song 2004; Yee & Jensen 2010). These systems may very well be young, albeit not younger than 10 Myr. Detection of He I emission at 5876Å and 6678Å for 8 systems (some of which had no lithium absorption) is also consistent with young ages for these stars.

The detection of lithium in at least 2/3 of the 24 spectroscopically observed stars suggests many of the other high-quality candidates may also be young stars, and perhaps others lie among the 100+ UV-excess stars with possible good UVW from which those candidates were drawn. Most of our objects lack RASS detections within $1'$ of their 2MASS coordinates; however, these tend to have upper limits of $\log L_X/L_{bol} \sim -3$, consistent with late-type stars that have been detected in the RASS. Because mid to late M-type stars have small L_{bol}, many would escape detection in RASS even if $\log L_X/L_{bol} \sim -3$. While deeper X-ray observations can be performed with Chandra or XMM, these will eventually cover only a few percent of the sky. This suggests that UV-selection criteria, such as the one we describe in this paper, may ultimately prove a more powerful tool than X-rays to identify nearby, young, low-mass stars.

Acknowledgements. We thank Simon Murphy for providing the high resolution spectrum for 2M1125–44 and the referee for useful suggestions. This publication makes use of data products from GALEX, operated for NASA by the California Institute of Technology, and the Two Micron All Sky Survey, which is a joint project of the University of Massachusetts and the Infrared Processing and Analysis Center/California Institute of Technology, funded by the National Aeronautics and Space Administration and the National Science Foundation. This work has used the SIMBAD and VizieR databases, operated at CDS, Strasbourg,

France. This research was supported by NASA Astrophysics Data Analysis Program grant NNX09AC96G to RIT and UCLA.

REFERENCES

Baraffe, I., Chabrier, G., Allard, F., & Hauschildt, P. H. 1998, A&A, 337, 403

Cardelli, J. A., Clayton, G. C., & Mathis, J. S. 1989, ApJ, 345, 245

Cutri, R. M., et al. 2003, The IRSA 2MASS All-Sky Point Source Catalog, NASA/IPAC Infrared Science Archive. http://irsa.ipac.caltech.edu/applications/Gator/

de Zeeuw, P. T., Hoogerwerf, R., de Bruijne, J. H. J., Brown, A. G. A., & Blaauw, A. 1999, AJ, 117, 354

The DENIS Consortium. 2005, VizieR Online Data Catalog, 2263, 0

Dommanget, J., & Nys, O. 2002, VizieR Online Data Catalog, 1274, 0

Dopita, M., Hart, J., McGregor, P., Oates, P., Bloxham, G., & Jones, D. 2007, Ap&SS, 310, 255

Findeisen, K., & Hillenbrand, L. 2010, AJ, 139, 1338

Gershberg, R. E., Katsova, M. M., Lovkaya, M. N., Terebizh, A. V., & Shakhovskaya, N. I. 1999, A&AS, 139, 555

Gliese, W., & Jahreiß, H. 1991, On: The Astronomical Data Center CD-ROM: Selected Astronomical Catalogs, Vol. I; L.E. Brotzmann, S.E. Gesser (eds.), NASA/Astronomical Data Center, Goddard Space Flight Center, Greenbelt, MD

Guinan, E. F., & Engle, S. G. 2009, IAU Symposium: The Ages of Stars, 258, 395

Kastner, J. H., Zuckerman, B., Weintraub, D. A., & Forveille, T. 1997, Science, 277, 67

Kastner, J. H., Huenemoerder, D. P., Schulz, N. S., Canizares, C. R., & Weintraub, D. A. 2002, ApJ, 567, 434

Krist, J. E., Stapelfeldt, K. R., Ménard, F., Padgett, D. L., & Burrows, C. J. 2000, ApJ, 538, 793

Kurosawa, R., Harries, T. J., & Symington, N. H. 2006, MNRAS, 370, 580

Mamajek, E. E., & Hillenbrand, L. A. 2008, ApJ, 687, 1264

Martin, D. C., et al. 2005, ApJ, 619, L1

Monet, D. G., et al. 2003, AJ, 125, 984

Morrissey, P., et al. 2007, ApJS, 173, 682

Natta, A., Testi, L., Muzerolle, J., Randich, S., Comerón, F., & Persi, P. 2004, A&A, 424, 603

Pourbaix, D., et al. 2004, A&A, 424, 727

Preibisch, T., & Feigelson, E. D. 2005, ApJS, 160, 390

Preibisch, T., & Mamajek, E. 2008, Handbook of Star Forming Regions, Volume II, 235

Reid, I. N., Hawley, S. L., & Gizis, J. E. 1995, AJ, 110, 1838

Riaz, B., Gizis, J. E., & Harvin, J. 2006, AJ, 132, 866

Röser, S., Schilbach, E., Schwan, H., Kharchenko, N. V., Piskunov, A. E., & Scholz, R.-D. 2008, A&A, 488, 401

Roeser, S., Demleitner, M., & Schilbach, E. 2010, AJ, 139, 2440

Sartori, M. J., Lépine, J. R. D., & Dias, W. S. 2003, A&A, 404, 913

Schmitt, J. H. M. M., Fleming, T. A., & Giampapa, M. S. 1995, ApJ, 450, 392

Song, I., Bessell, M. S., & Zuckerman, B. 2002, ApJ, 581, L43

Song, I., Zuckerman, B., & Bessell, M. S. 2003, ApJ, 599, 342

Stauffer, J., et al. 2010, arXiv:1006.2441

Torres, C. A. O., Quast, G. R., da Silva, L., de La Reza, R., Melo, C. H. F., & Sterzik, M. 2006, A&A, 460, 695

Torres, C. A. O., Quast, G. R., Melo, C. H. F., & Sterzik, M. F. 2008, Handbook of Star Forming Regions, Volume II, 757

Walkowicz, L. M., & Hawley, S. L. 2009, AJ, 137, 3297

White, R. J., & Basri, G. 2003, ApJ, 582, 1109

Yee, J. C., & Jensen, E. L. N. 2010, ApJ, 711, 303

Zacharias, N., et al. 2010, AJ, 139, 2184

Zickgraf, F.-J., Krautter, J., Reffert, S., Alcalá, J. M., Mujica, R., Covino, E., & Sterzik, M. F. 2005, A&A, 433, 151

Zuckerman, B., & Song, I. 2004, ARA&A, 42, 685

Table 1. GALEX Searches

Region[a]	RA	Dec	Radius	GALEX/2MASS sources
TWA	11h30m	−35°	18°	47,101[b]
LCC 1	10h56m	−63°	15°	381,385
LCC 2	12h50m	−60°	18°	
UCL 1	14h45m	−45°	18°	548,324
UCL 2	16h20m	−33°	18°	

[a]TWA: TW Hydra Association; LCC: Lower Centaurus-Crux; UCL: Upper Centaurus-Lupus

[b]Only the TWA search required detection in both NUV and FUV.

Note. — List of all searches performed. See also Fig. 6. Number of stars quoted for LCC 1 region also includes stars in LCC 2; similarly for UCL 1 and UCL 2.

Table 2. UV Selected Objects

RA (deg)	Dec (deg)	2MASS Designation	μ_α (mas/yr)	μ_δ (mas/yr)	J–K	NUV-J	Spectral Type	D (pc)	RV Range (km/s)	log L_X/L_{bol}
156.337	-42.6983	10252092–4241539	-47.	-2.	0.91	10.04	M2-M2.5	91.	10:30	-3.03
156.509	-41.0983	10260210–4105537	-46.	-3.	0.9	9.58	M3-M3.5	67.	8:31	-3.24
165.8988	-30.4137	11033571–3024494	-36.	-18.	0.84	9.34	M0	126.	0:26	< -3.57
171.448	-44.1741	11254754–4410267	-37.	-18.	0.86	10.26	M4-M4.5	75.	2:27	-2.33
172.812	-48.4411	11311482–4826279	-40.	-6.	0.87	9.03	M3-M3.5	130.	17:26	< -3.24
174.079424	-52.515057	11361906–5230542	-31.	-10.	0.86	10.12	M3-M3.5	123.	4:29	-2.80
176.596286	-52.647766	11462310–5238519	-46.	-14.	0.89	9.88	M4.5-M5	85.	3:28	< -2.97
179.866105	-45.172005	11592786–4510192	-44.	-24.	0.87	10.15	M4.5-M5	55.	5:21	-2.99
179.99	-26.3761	11595770–2622340	-32.	-17.	0.85	9.20	M3-M3.5	113.	-2:23	< -3.35
181.698	-19.3481	12064743–1920531[a]	-56.	-7.	0.77	9.50	K7-M0	71.	2:11	< -3.57
182.1542	-21.45811	12083700–2127291[a]	-73.	-36.	0.81	9.85	M3	60.	-4:21	< -2.92
184.598	-35.2527	12182363–3515098	-28.	-13.	0.82	9.88	M0.5-M1	101.	2:22	-3.19
184.973163	-74.33593	12195355–7420093	-34.	-14.	0.89	10.81	M3.5-M4	104.	5:28	-3.03
186.714	-33.2701	12265135–3316124	-62.	-25.	0.91	9.34	M5	65.	-2:23	< -3.10
186.855	-45.6685	12272529–4540065	-30.	-14.	0.76	8.89	K7-M0	149.	2:25	-3.11
187.521722	-44.04332	12300521–4402359	-44.	-18.	0.88	10.53	M4.5-M5	69.	2:24	< -3.25
190.225488	-45.27367	12405411–4516252	-35.	-13.	0.91	10.92	M3-M3.5	124.	2:26	< -3.19
192.215415	-45.939037	12485169–4556205	-27.	-14.	0.9	10.07	M4.5-M5	121.	0:23	< -2.76
192.698969	-42.53022	12504775–4231487	-34.	-18.	0.82	9.88	M4.5-M5	120.	-1:26	< -2.76
194.322195	-46.447998	12571732–4626527	-31.	-20.	0.87	10.35	M3.5-M4	146.	2:23	< -2.95
196.442675	-44.293636	13054624–4417370	-35.	-16.	0.89	10.49	M3-M3.5	143.	6:22	-2.78
196.632647	-44.919258	13063183–4455093	-29.	-13.	0.87	10.41	M2-M2.5	138.	0:26	< -3.28
197.870938	-42.878288	13112902–4252418	-35.	-19.	0.9	10.51	M2-M2.5	121.	0:25	-2.93

Continued on next page

Table 2—Continued

RA (deg)	Dec (deg)	2MASS Designation	μ_α (mas/yr)	μ_δ (mas/yr)	J–K	NUV-J	Spectral Type	D (pc)	RV Range (km/s)	log L_X/L_{bol}
200.17506	-46.976494	13204201–4658353	-29.	-20.	0.91	9.69	M4-M4.5	126.	-3:21	< -2.92
201.775952	-43.506329	13270622–4330227	-35.	-17.	0.86	10.16	M4.5-M5	118.	0:24	< -2.80
202.060031	-39.487438	13281440–3929147	-28.	-32.	0.91	10.60	M4-M4.5	84.	-2:11	< -3.22
202.126198	-39.568535	13283028–3934067	-32.	-14.	0.91	9.69	M4-M4.5	134.	0:21	< -2.86
202.135325	-42.695457	13283247–4241436	-44.	-36.	0.93	10.23	M3-M3.5	111.	3:18	< -3.27
203.373612	-37.88876	13332966–3753195	-23.	-20.	0.91	10.45	M4-M4.5	143.	-7:16	< -2.89
203.880003	-42.696892	13353120–4241488	-26.	-23.	0.94	10.11	M4-M4.5	123.	-5:17	< -3.02
204.409991	-47.608257	13373839–4736297	-32.	-23.	0.91	9.47	M4.5-M5	126.	0:23	< -2.70
207.22411	-48.84594	13485378–4850453	-33.	-18.	0.86	10.68	M3.5-M4	146.	4:22	< -3.02
207.940297	-37.700115	13514567–3742004	-26.	-36.	0.92	10.25	M2-M2.5	119.	-9:13	< -3.43
208.190309	-49.642429	13524567–4938327	-37.	-17.	0.84	10.32	M4.5-M5	112.	1:22	< -2.75
210.906607	-50.179924	14033758–5010477	-33.	-18.	0.86	10.55	M4-M4.5	98.	-3:17	< -3.16
211.712131	-50.98185	14065091–5058546	-28.	-24.	0.9	10.83	M4-M4.5	121.	-3:18	< -3.04
216.715646	-33.826576	14265175–3349356	-28.	-32.	0.9	10.72	M3.5-M4	139.	-5:14	< -3.05
218.440042	-31.41147	14334561–3124412	-20.	-30.	0.89	9.54	M4.5-M5	97.	-8:5	< -2.88
219.305101	-34.155811	14371322–3409209	-32.	-31.	0.89	9.81	M3-M3.5	145.	-3:15	< -3.17
222.245008	-32.402317	14485880–3224083	-34.	-32.	0.85	9.84	M4.5-M5	132.	-4:14	-2.38
222.639972	-34.341827	14503359–3420305	-29.	-31.	0.88	9.45	M4-M4.5	142.	-11:7	< -2.90
226.646079	-36.658264	15063505–3639297	-34.	-25.	0.93	9.87	M5-M5.5	118.	-4:13	< -2.58
227.068891	-34.579636	15081653–3434466	-31.	-32.	0.91	9.87	M4-M4.5	140.	-5:12	< -2.86
228.050838	-25.952211	15121220–2557079	-20.	-33.	0.89	10.88	M2-M2.5	99.	-14:3	< -3.58
231.234692	-29.413294	15245632–2924478	-26.	-32.	0.88	10.32	M4.5-M5	116.	-10:6	< -2.76
232.789928	-35.082542	15310958–3504571	-34.	-30.	0.92	10.67	M4.5-M5	70.	-10:6	< -3.12

Continued on next page

Table 2—Continued

RA (deg)	Dec (deg)	2MASS Designation	μ_α (mas/yr)	μ_δ (mas/yr)	J–K	NUV-J	Spectral Type	D (pc)	RV Range (km/s)	log L_X/L_{bol}
233.912086	-38.210953	15353890–3812394	-30.	-38.	0.89	10.31	M4-M4.5	126.	-5:11	< -2.94
234.257429	-36.814156	15370178–3648509	-16.	-34.	0.88	9.80	M4-M4.5	108.	-11:5	< -3.14
236.847334	-36.736374	15472336–3644109	-26.	-29.	0.87	9.81	M4.5-M5	135.	-7:9	< -2.68
236.852005	-36.726772	15472448–3643363	-24.	-30.	0.86	9.27	M3-M3.5	130.	-8:8	-3.00
238.948557	-36.566711	15554765–3634001	-30.	-37.	0.88	10.68	M4-M4.5	103.	-8:7	-2.86
242.36897	-32.104786	16092855–3206172	-12.	-34.	0.9	9.85	M4.5-M5	115.	-13:2	< -2.79
242.478602	-30.982832	16095486–3058581	-18.	-32.	0.91	10.48	M2-M2.5	130.	-11:4	< -3.36
244.974809	-31.901608	16195395–3154057	-24.	-26.	0.88	10.54	M3-M3.5	144.	-9:5	-2.86

[a]For these objects distance and RV ranges are quoted using 100-Myr isochrones.

Note. — Spectral types are obtained from photometric colors. RV Range is the range of radial velocities that give good UVWs (see Section 2.2 for more details). Unless otherwise noted in footnote *a*, all distances are calculated using 10-Myr isochrones and have uncertainties of 20%. Upper limits for the last column are derived assuming $F_X = 2 \times 10^{-13}$ ergs cm^{-2} s^{-1}, the characteristic RASS flux limit (Schmitt et al. 1995).

Table 3. Spectroscopic Results

Target	Spectral Type	Dist. (pc)	He I 5876Å	Hα 6563Å	He I 6678Å	Li I 6708Å
10252092–4241539	M1	91		-3.6 ± 0.6		490 ± 30
10260210–4105537	M1	67		-7.4 ± 0.3		500 ± 70
11254754–4410267	M4	75	-0.8 ± 0.2	-8.2 ± 0.2	-50 ± 30	< 30
12265135–3316124	M5	65	-6.4 ± 0.2	-64.0 ± 4.0	-1200 ± 200	410 ± 40
				-51.1 ± 7.0	-670 ± 110	573 ± 50
11311482–4826279	M3	130		-7.9 ± 0.5		60 ± 20
11462310–5238519	M4.5	85		-10.1 ± 0.5		66 ± 20
11592786–4510192[a]	M4.5	55		-8.18 ± 0.3		527 ± 50
12300521–4402359	M4	69		-7.2 ± 0.2		503 ± 30
13112902–4252418	M1.5	121		-4.2 ± 0.2		255 ± 20
13281440–3929147	M4	84		-8.7 ± 0.2		165 ± 20
13283247–4241436	M2	111		-3.8 ± 0.2		180 ± 20
13373839–4736297	M3.5	126	-1.3 ± 0.1	-13.7 ± 0.2	-115 ± 50	308 ± 40
13514567–3742004	M1	119		-2.2 ± 0.1		200 ± 10
13524567–4938327	M4.5	112		-8.5 ± 0.1		517 ± 50
14265175–3349356	M3.5	139	-0.6 ± 0.1	-10.2 ± 0.4	-24 ± 10	< 50
14371322–3409209	M3.5	145		-9.7 ± 0.6		< 30
14485880–3224083	M4.5	132		-11.8 ± 0.4		< 60
14503359–3420305	M3.5	142	-1.0 ± 0.1	-10.5 ± 0.4	< -30	< 80
				-6.9 ± 0.6		< 50
15063505–3639297	M5	118	-1.9 ± 0.3	-12.1 ± 0.3	-44 ± 20	446 ± 90
15081653–3434466	M3.5	140		-7.8 ± 0.5		< 60
15245632–2924478	M4.5	116		-8.7 ± 0.6		< 100
15310958–3504571	M4.5	70	-2.0 ± 0.2	-17.4 ± 0.3	-145 ± 60	258 ± 40
15353890–3812394	M4	126		-5.97 ± 0.3		388 ± 40
15554765–3634001	M3.5	103	-1.0 ± 0.2	-13.6 ± 0.2	-39 ± 10	184 ± 20

[a]The strong lithium line detected in 2M1159–45 was initially and independently seen in previous observations at Siding Spring Observatory (Zuckerman et al. 2010, submitted to ApJ).

Note. — The first four objects are from the TWA search, the rest are from the Sco–Cen searches (see Table 1). Some candidate objects found in the Sco–Cen searches may be TWA candidates (see Fig. 6). Spectral types are estimated using the TiO5 index as described in Reid et al. (1995) and distances assume the star is ∼10 Myr old. He I (5876Å) and Hα equivalent widths are measured in Å, all others are in milliÅ, with negative equivalent widths denoting emission lines. Upper limits (3-σ) are provided when a line is not detected. The extra row below 2M1226–33 and 2M1450–34 are values measured from the R7000 spectra.

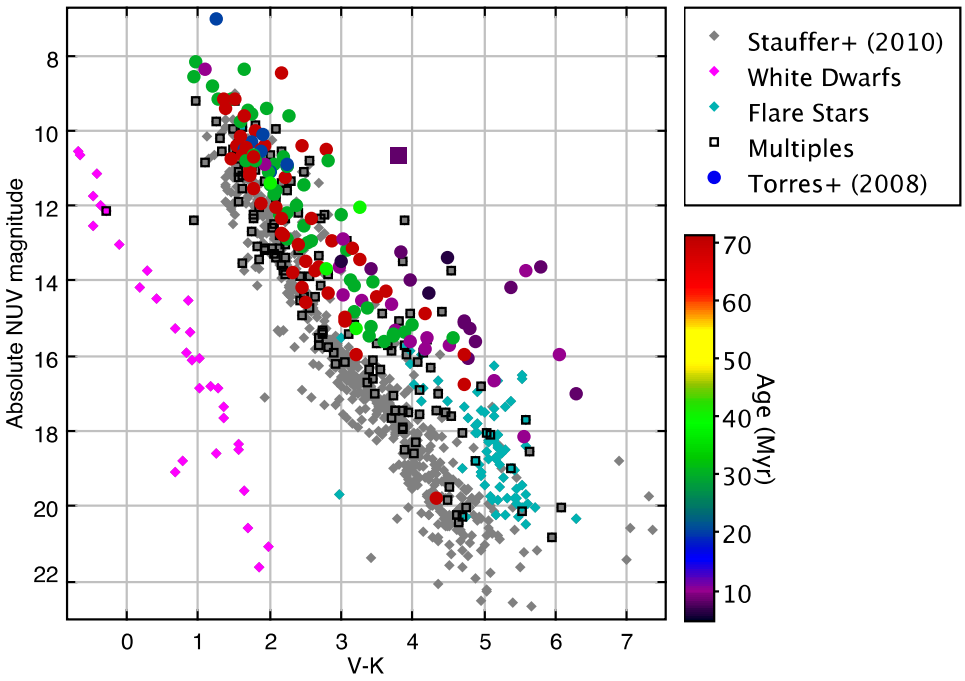

Fig. 1.— The circles, color-coded by age, are objects in Torres et al. (2008) that were matched in GALEX. TW Hya is displayed as a large square. All other symbols are stars from Stauffer et al. (2010), which provides accurate coordinates for most of the stars in the Gliese catalog (Gliese & Jahreiß 1991). Different symbols highlight some of the known multiple, white dwarfs, and flare star systems. The grey symbols left of the main sequence are likely to have incorrect distances, V-band magnitudes, or both (some such systems were corrected when updated information was available). In general, the Gliese low-mass stars (K5/K7 and later, V–K$\geq$ 3) are older and fainter in NUV than stars in young associations by 2 magnitudes on average, the notable exception being flare stars and some multiples. Multiples among the Torres et al. (2008) stars are not labeled.

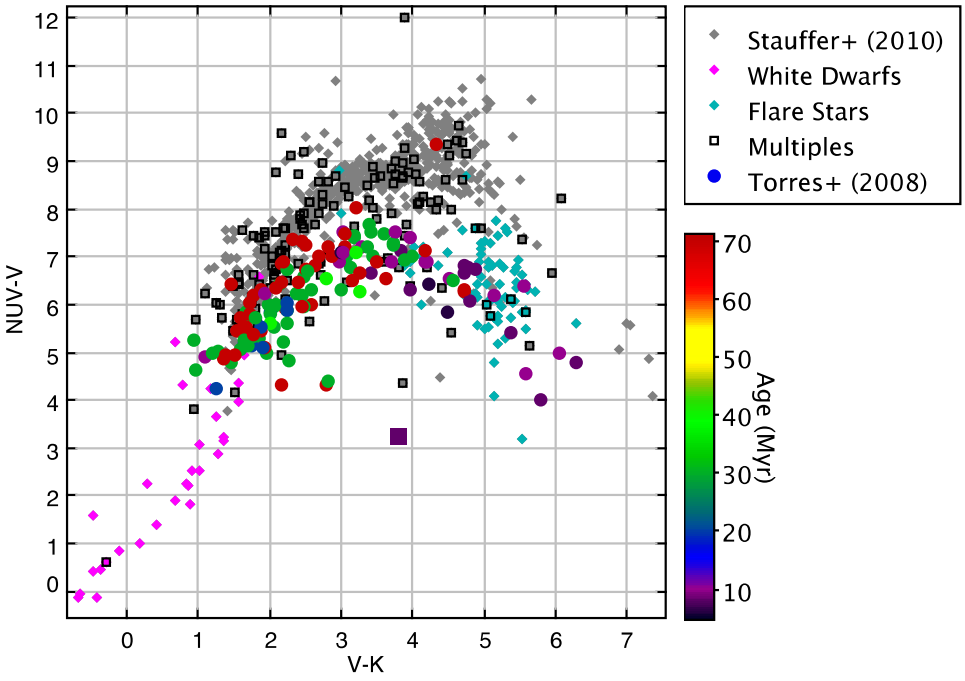

Fig. 2.— When plotting the members of young associations and the Gliese stars (see Fig. 1) in NUV–V color, the distinction between old and young, late-type (K5/K7 and later, V–K$\geq$ 3) stars become more readily apparent. Objects with lower NUV–V are brighter in NUV and generally younger. TW Hya is displayed as a large square. Putative AB Dor member BD +01 2447 is located at V–K$\sim$4.3 and NUV–V$\sim$9.4. We comment on both these systems in § 3.4.

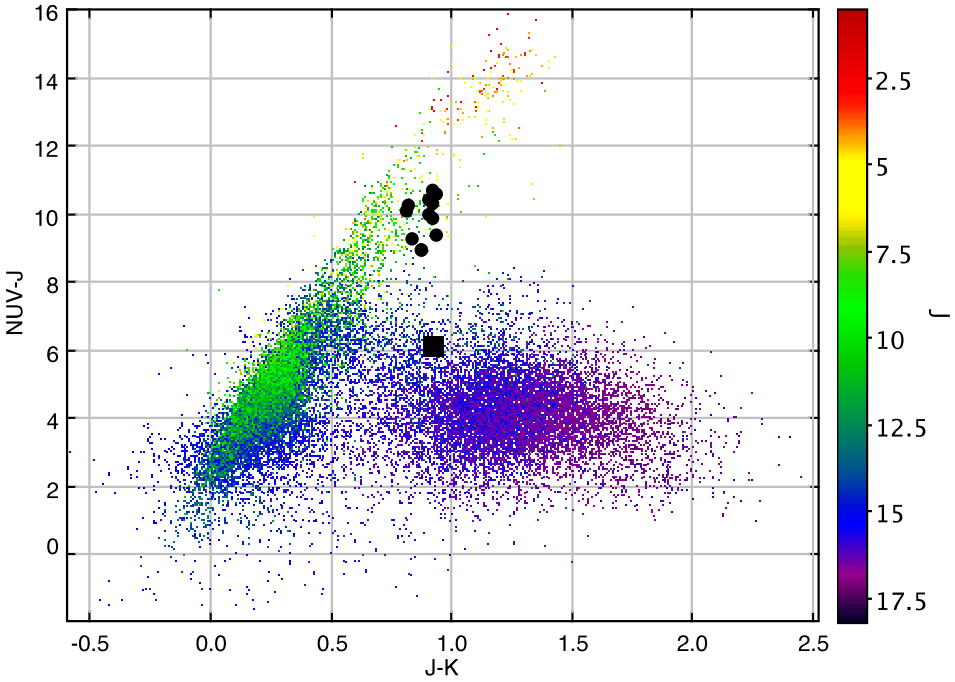

Fig. 3.— Color-color plot for the TWA search. The colored dots (color based on J magnitude) are the GALEX/2MASS sources, while the larger black dots are known TWA members from Torres et al. (2008). The TWA member labeled as a large square is TW Hya itself. The cloud of sources between about 0.5<J–K<2 and 2<NUV–J<7 are generally distant galaxies and most can be removed from this plot by imposing a cut of J≤14. All TWA objects lie somewhat below the line of stellar sources (ie, they have UV excesses; see Fig. 4).

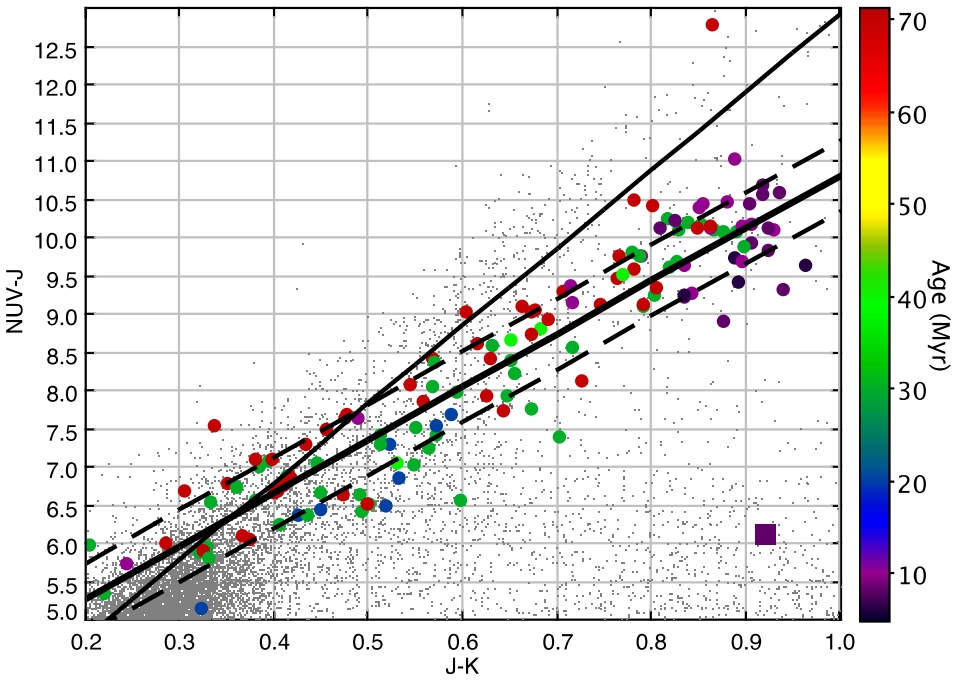

Fig. 4.— The grey dots are the GALEX/2MASS sources in the vicinity of TWA (see the first line entry to Table 1); those near the bottom right are the upper portion of the galaxy distribution (see Fig 3). The colored circles are for stars in Torres et al. (2008), where the color corresponds to the age of the association or moving group. TW Hya is the large purple square. The thin solid line represents the relations in Findeisen & Hillenbrand (2010) and defines the stellar sequence as extrapolated from early-type stars. The thick solid line is the best-fit line to the young star sample and demonstrates (as in Figs 1 and 2) how young late-type stars stand out. Dashed lines outline the 1-σ variation among the young stars.

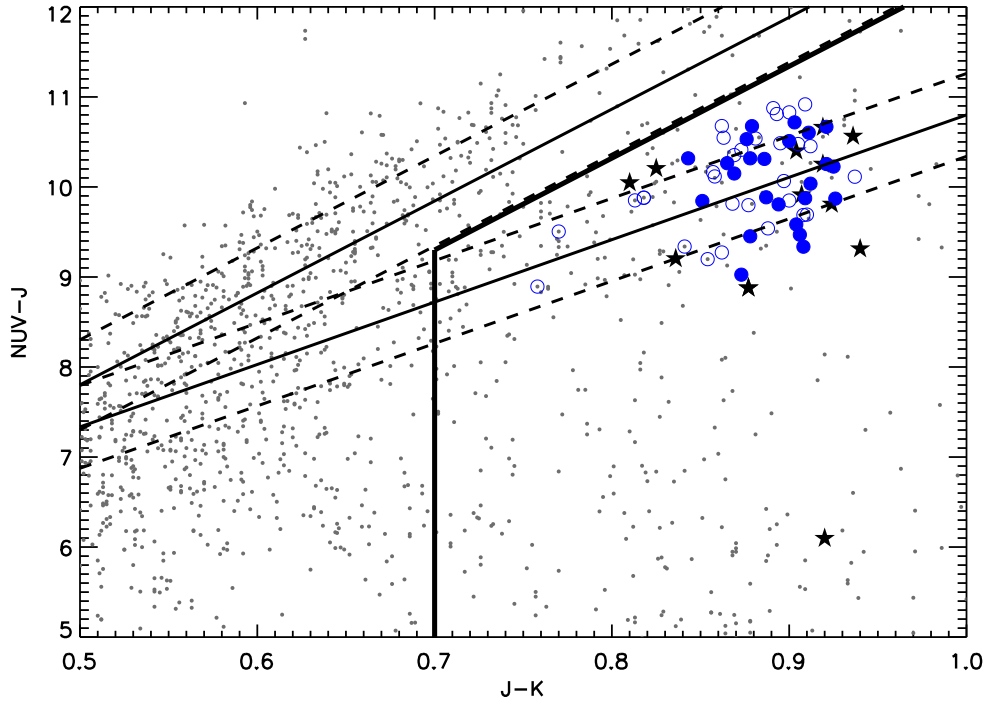

Fig. 5.— Our 54 UV-excess candidate stars are plotted as circles with filled circles denoting our spectroscopic sample. TWA members known previous to our study (namely, those listed in Torres et al. 2008) are plotted with star symbols. Our selection criteria are denoted by the thick black lines; the thin solid lines denote the relation in Findeisen & Hillenbrand (2010) for the stellar sequence and our best-fit line to the young stars (see Fig. 4). Both have their associated 1-σ errors as dashed lines. The grey dots are the GALEX/2MASS sources in the vicinity of TWA with J$\leq$14, which removes many of the galaxies. While we select all objects that satisfy our color-color criteria, most do not have proper motions, distances, or UVW consistent with those of young stars (see Sections 2.2 and 3.1).

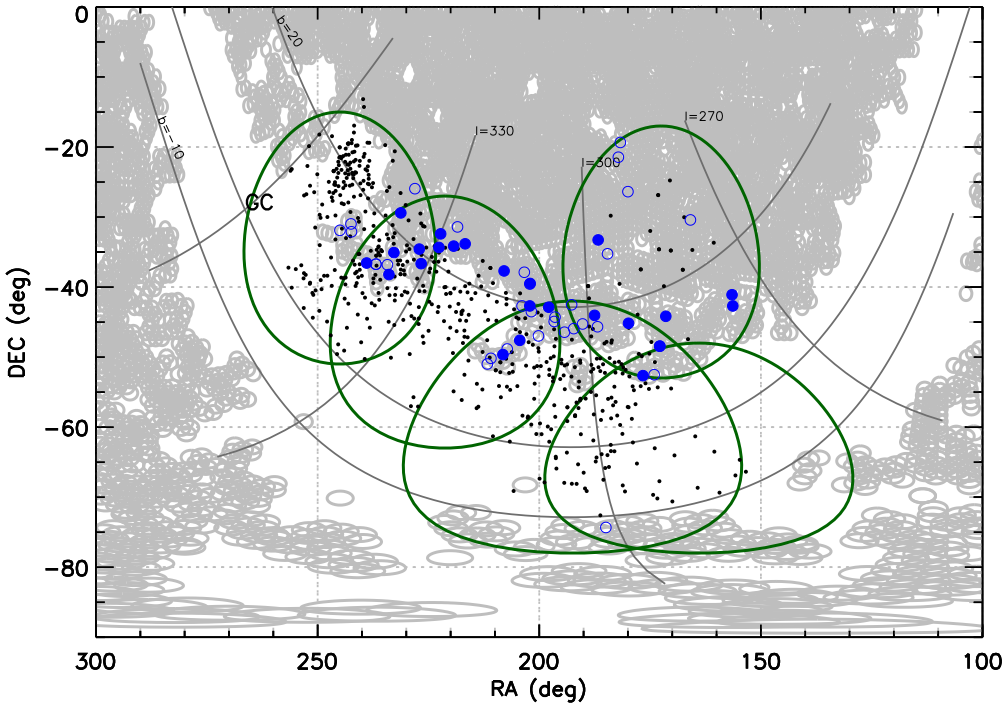

Fig. 6.— Search regions (see Table 1) for the Sco–Cen and TW Hya Associations. Dots are candidate TWA, Upper Scorpius, UCL, and LCC members from Torres et al. (2008) and de Zeeuw et al. (1999). Circles denote candidate objects (Table 2); those we have spectra for are displayed as filled circles (Table 3). Our search regions encompasses all known members and candidates for these regions and extends somewhat beyond in order to explore for more distant members. All GALEX fields in the GR4/5 database are denoted in gray. Note that GALEX avoids the galactic plane (generally within 10°) so that our coverage is better on the northern parts of our searched fields.

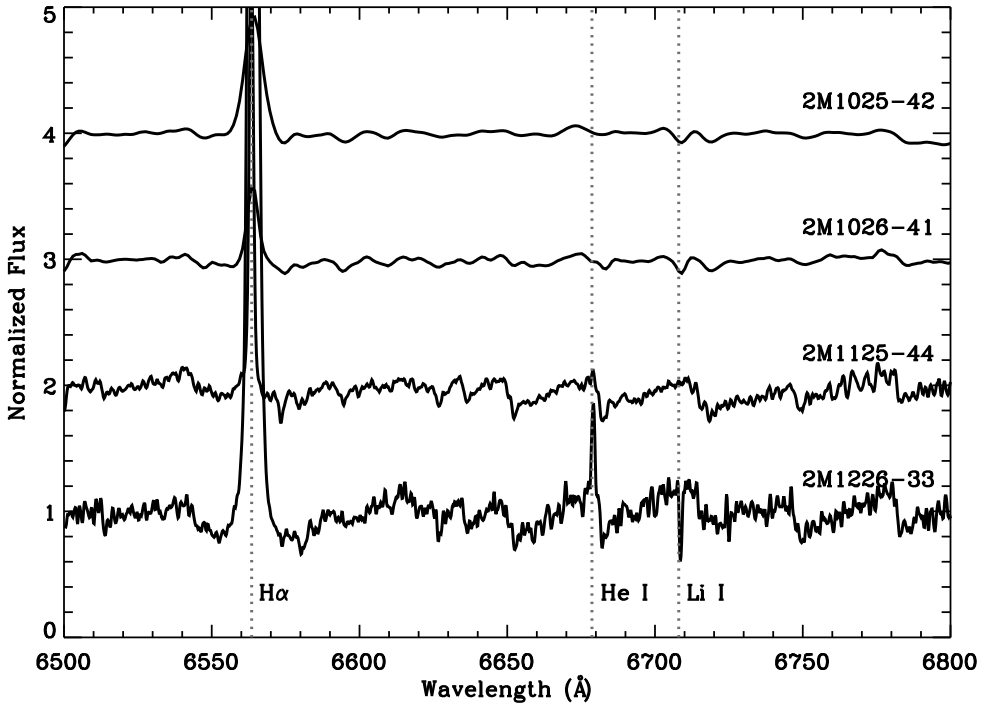

Fig. 7.— R_{3000} WiFeS spectra for our 4 TWA candidates. The spectra for 2M1125-44 and 2M1226–33 were obtained with R=7000.

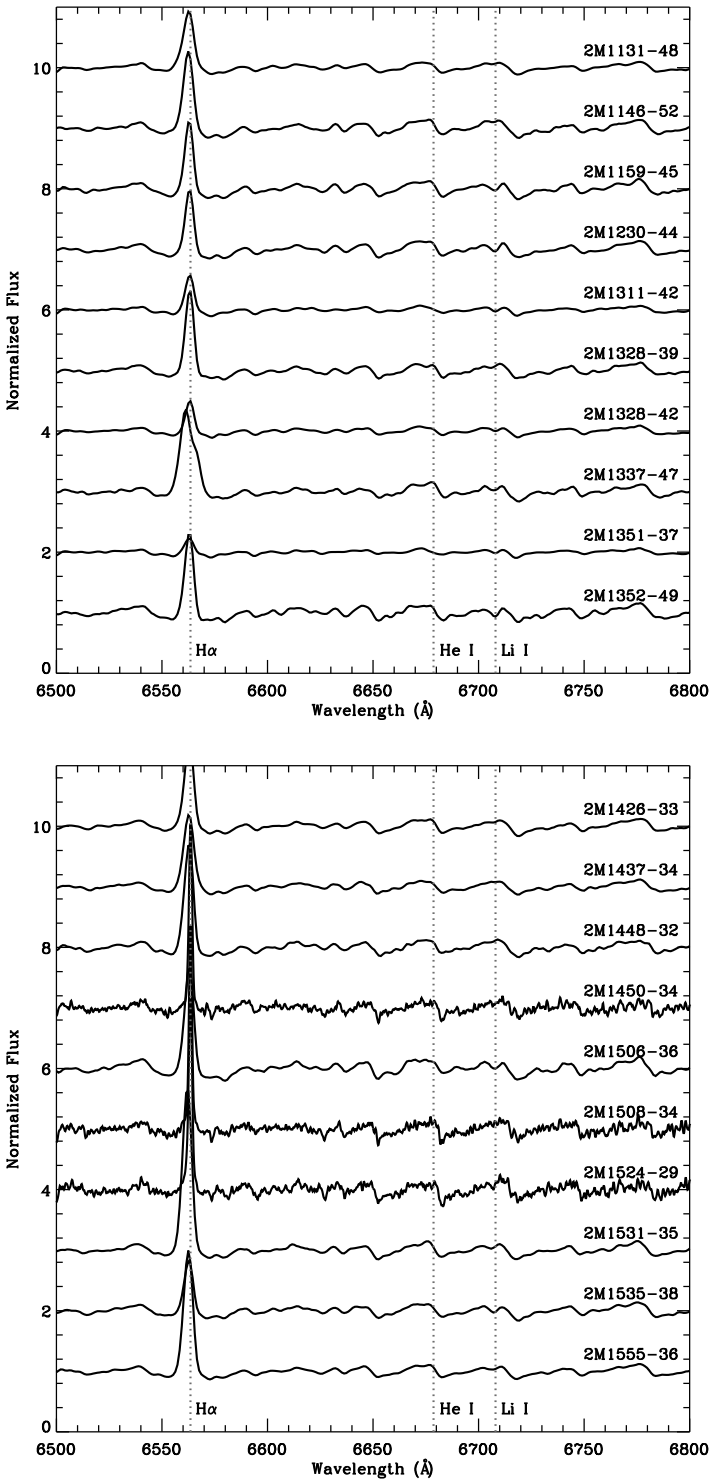

Fig. 8.— WiFeS spectra for our 20 Sco–Cen candidates. 2M1337-47, which shows asymmetry in its (blue-shifted) Hα profile, also shows a double peak for the other Hydrogen lines possibly due to accretion from a surrounding disk (Kurosawa et al. 2006). The spectra for 2M1450–34, 2M1508–34, and 2M1524–29 were obtained with R=7000.